CrossMark

THEMATIC ISSUE

Mechanical and permeability characteristics of rock under hydro-mechanical coupling conditions

Lu Wang · Jian-feng Liu · Jian-liang Pei ·
Hui-ning Xu · Yu Bian

Abstract A study on the mechanical characteristics and permeability properties of sandstone and limestone from a coal mine under 3D stresses has been carried out with the MTS815 rock mechanics test system, and the characteristics of mechanics and permeability before and after the rock failure under hydro-mechanical coupling conditions have been analyzed and discussed. The research revealed the difference of mechanics and permeability before and after the rock failure and obtained the relationship among the strength, deformation and differential water pressure. It also obtained the correlation among the permeability and stress, strain and revealed the features of fractures which influenced the correlation. The results show that there are obvious weakening effects of differential water pressures on the mechanical properties after the rock damages; the permeability of rock mass in practical engineering is mainly controlled by the features of fractures; the permeability has an negative index correlation with the axial strain ε_1, and has a power function correlation with the mean stress $\sigma_m (\sigma_m = (\sigma_1 + 2\sigma_3)/3)$; for fractured limestone and coarse sandstone, the permeabiity will tend to be stable gradually when the mean stress reaches or exceeds a certain value σ_{ml}.

Keywords Hydro-mechanical coupling · Rock · Strength · Deformation · Permeability

L. Wang · J. Liu (✉) · J. Pei · H. Xu · Y. Bian
State Key Laboratory of Hydraulics and Mountain River
Engineering, Sichuan University, Chengdu 610065, China
e-mail: ljfscu@163.com; liujf@scu.edu.cn

Introduction

The problem of groundwater and its seepage is important and inevitable in coal mines. The rock mass is under the different states of stress and pore water pressure at different depth. In the process of mining, the structure, permeability and mechanical properties of rock masses will be changed by the engineering behaviors which disturb the original stress field and seepage field. The properties and mechanical parameters obtained under the conventional conditions are not applicable for the rock mass engineering under the hydro-mechanical coupling conditions. So the study on the permeability and mechanical characteristics of rocks (including intact rocks and fractured rocks) under hydro-mechanical conditions is significant.

Water is one of the factors influencing the mechanical characteristics of rocks. The weaken effect of water on the strength and deformation of rocks has been revealed in some experimental researches (Lajtai et al. 1987; Masuda 2001), and the weaken effect is closely related to the mineral composition and the water content (Chai et al. 2014; Vásárhelyi and Ván 2006; Wasantha and Ranjith 2014). In addition, the weaken effect will be more significant if the rock is under the water pressure (Li et al. 2013). In the coal mining engineering, there may be differential water pressure in rocks because of the excavation. Therefore, the rocks are under the water pressure–flow coupling conditions, and the weaken effect on mechanical characteristics may become more complicated. However, there are few researches on this problem now.

The permeability of rocks is as important as the mechanical characteristics under the hydro-mechanical coupling conditions. Some researches focus on the permeability evolution laws in the complete stress–strain process (Li et al. 1997; Helland and Raab 2001; Wang and

Park 2002; Wang et al. 2014), and point out that the permeability evolution shows the phases characteristics during the process of stress and strain. For the porous rocks, the permeability is related to the porosity, but the correlation between the permeability and porosity before the dilatancy is different from that after the dilatancy by the reason of the effect of shear band (Zhu and Wong 1996; David et al. 2001). In order to make the permeability evolution quantitative and reveal the relationship between the permeability and mechanical behaviors, some equations of permeability and strain have been founded based on tests (Li et al. 1994; Wang and Xu 2013; Zhang et al. 2013). The relationship between the permeability and stress has been studied as well and some qualitative and quantitative relationships have been obtained (Jiang et al. 2002; Tang et al. 2002; Peng et al. 2003).

Compared with the intact rock in the laboratory, the engineering rock mass has different kinds of structural planes which connect with each other to form the main seepage channels. So the permeability of fractured rocks is much higher than that of intact rocks (Oda et al. 2002). The relational expressions between the permeability and stress of a single fracture were studied early on (Jones 1975; Gale 1982; Barton et al. 1985). Based on some tests, the permeability of fractures is bound up with the confining pressures and fluid pressures (Gangi 1978; Kranzz et al. 1979; Walsh 1981), and the permeability has a close relationship with the lateral strain and volumetric strain (Zoback and Byerlee 1975; Chang et al. 2004). Nonetheless, the permeability of fractured rocks is closely related to the spatial geometric features of fractures, and so the relationship between the permeability and strain does. However, the research on the relationship between the permeability and strain based on the fracture features of rocks is seldom seen.

From the above, the objects of study on the permeability of rocks are mainly intact rock specimens and the rock specimens with single fracture, which differs from the engineering rock masses to some extent. And most researches focused on the effects of the stress and deformation of rocks on the permeability and the effects of pore pressure (or average pore pressure) on the properties of rocks, but distribution of pore pressures in the rocks under differential water pressures and the effect mechanism of differential water pressures are complex, which make it necessary to pay attention to the effects of differential water pressures on the rock mechanics. In this study, intact rock specimens of limestone and coarse sandstone are loaded to failure firstly under the hydro-mechanical coupling conditions, and then the hydro-mechanical coupling tests on the fractured rocks which are prepared from the intact rocks in the previous process are carried out. Based on these tests, the effects of differential water pressure on

rock mechanical characteristics are discussed; the permeability evolutions of intact rocks and fractured rocks are analyzed to reveal the difference between them; based on the analyses and the fractures features of fractured rocks, the correlative equations of permeability–strain and permeability–stress under the hydro-mechanical coupling conditions are founded.

Specimen and experimental method

Specimen and experimental system

The rock samples of limestone and coarse sandstone are from a coal mine in Ningwu Basin which is in Shanxi province, China. Ningwu Basin was formed by tectonic movement in the late Paleozoic era and affected by some orogenic movements in the late Mesozoic. During this process, many complicated fractures were induced by multiphase tectonic stresses. The average saturation densities of limestone with the porosity of 3.6 % and coarse sandstone with the porosity of 18.2 % are 2.64 g/cm^3 and 2.64 g/cm^3, respectively. Specimens were prepared following the Standard for Test Methods of Engineering Rock Mass (GB/T50266-2013), with the diameter of 50 mm and the height of 100 mm. The specimens were saturated before tests.

The hydro-mechanical coupling tests were conducted on the MTS815 Flex Test GT rock mechanics test system. The axial deformation of the specimen was measured by an axial extensometer (−2.5 to 5 mm) and the circumferential deformation was measured by an extensometer (−2.5 to 8 mm) with the measurement and control precision of 0.5 % RO. The loading and measurement during the testing process were controlled by the computer program which is stable and accurate. The real-time test data were all measured by the high- precision sensor and recorded by computer automatically.

Experimental method

Taking account of the fractures presented in rocks in situ, which cause the rock mechanical and permeability properties to be much different from that of the relatively intact specimens in laboratory, the test scheme is designed as follows to simulate these fractured rocks: first, intact rock specimens are loaded under the hydro-mechanical coupling conditions to obtain the permeability evolution in the deformation process and the fractured rock specimens; then the hydro-mechanical coupling tests are performed on these fractured rocks. The permeability during the tests is measured by the transient pulse technique (Brace et al. 1968; Hsieh et al. 1981; Neuzil et al. 1981), which measures the decay of a pressure differential across the
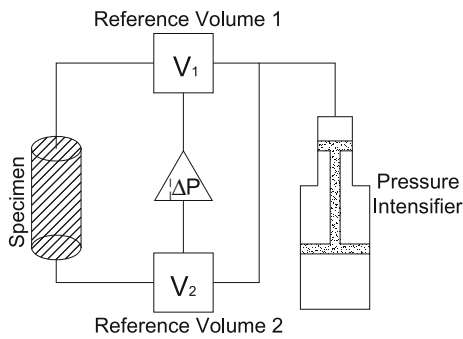
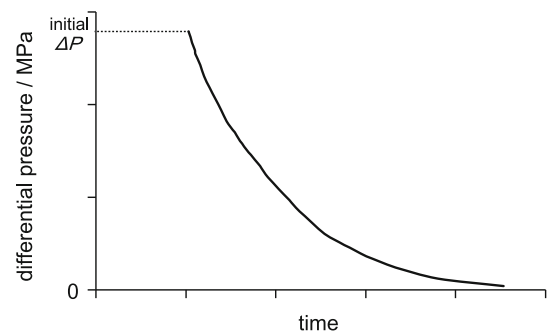Fig. 1 Simplified schematic of transient permeability system

Fig. 2 Installation of specimen

Fig. 3 Curves of differential pressure and time

Table 1 Values of confining pressure σ_3, water pressure P_w and differential water pressure ΔP_w

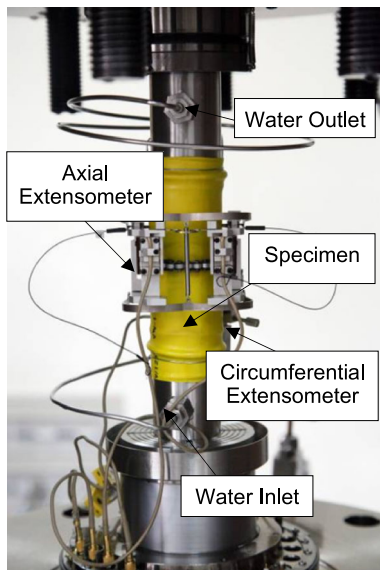| Specimen	Test procedure	σ_3/MPa	$P_w(\Delta P_w)$/MPa
Coarse sandstone	Part I	16	3
	Part II	4	3
		12	3, 6, 9
		16	3, 6, 9, 12, 15
Limestone	Part I	16	6
	Part II	4	3
		8	3, 6
		12	3, 6, 9
		16	3, 9, 12, 15

specimen as a function of time by the transient permeability system (Fig. 1) to obtain the permeability.

Based on the test scheme, a whole test of a specimen consists of two parts (Part I and Part II). After the installation of the saturated specimen into the test system (Fig. 2), the test is conducted according to the following procedures:

Part I is the test on intact specimens under hydro-mechanical coupling conditions. First, the confining pressure σ_3 and water pressure $P_w(P_w < \sigma_3)$ are loaded to the predetermined value successively with a loading rate of 3 MPa/min. In order to obtain the permeability under the condition of hydrostatic pressure, lower the water pressure at the top of the specimen to form a differential pressure ΔP_w, which makes the water flow through the specimen. Then the differential pressure decreases over time until equilibrium is attained again (Fig. 3). This process is monitored and recorded by computer automatically. Secondly, the water pressure is restored at the bottom of the specimen to the initial value and the water pressure is released at the top to create a constant differential water pressure across the specimen during the axial stress loading process, and then the axial stress σ_1 is applied to the next stress level. Thirdly, the water pressure is applied to the top of the specimen to equalize the bottom pressure, and then to lower the upper water pressure suddenly to measure the permeability under the present stress level. The second and third steps are repeated until the residual stress is attained. During the axial stress loading process, in order to avoid the sudden rock failure and obtain the post-peak mechanical behavior and permeability, the axial stress is firstly loaded at a rate of 30 kN/min and then a lateral deformation rate of 0.02 mm/min is maintained after the yield stress.

Part II is the test on fractured rock specimens under hydro-mechanical coupling conditions. Based on the Part I test, the fractured rock specimen is obtained. Following the Part I test, the axial stress σ_1 is adjusted to the water pressure P_w and confining pressure σ_3 to the predetermined value successively and the permeability is measured under the condition of hydrostatic pressure in the same way as the Part I test. Then the axial stress is loaded at a lateral deformation rate of 0.04 mm/min to each stress level under

which the permeability is measured as the Part I test until the peak stress is reached.

The conditions of confining pressure σ_3, water pressure P_w and differential water pressure ΔP_w in the tests are listed in Table 1. The values of P_w are equal to the values of differential water pressure ΔP_w.

Mechanical characteristics

Properties of stress–strain curves

The stress–strain curves of intact rocks are significantly different from that of fractured rocks (Fig. 4). The stress–strain curves of intact rocks exhibit the five phases of the idealized stress–strain curve: the initial deformation phase, elastic deformation phase, plastic deformation phase, strain-softening phase and residual phase. Whereas there are only the first three phase in the curves of fractured rocks. The slope and peak of the curves of intact rocks are much larger than that of fractured rocks, which indicates that the fractures seriously weaken the stiffness and strength of rocks. Figure 4 shows that the axial deformations of intact rocks and fractured rocks are mostly greater than the lateral deformations. Based on the volumetric strain–stress curves, the volume of intact limestone specimen shrinks before the peak stress and then the dilatation occurs; whereas the volume of intact coarse sandstone specimen is compressed during the complete process; the dilatation of the fractured limestone specimen is more obvious than that of the coarse sandstone. These deformation characteristics of fractured rocks are closely related to the fractures properties.

Figure 4a, c shows the effect of differential water pressures on fractured rocks. The slope and peak of the curves of fractured rocks both reduce and the volumetric dilatancy being stronger with the increasing differential water pressure, which indicates the obvious weakening effect of water pressures on the deformation and strength of rocks. As is known, the differential water pressure reduces the effective stress of rocks, which affects the stress condition. At the same time, the microstructures and deformation of fractured rocks are closely related to the stress conditions. So the differential water pressure has significant influence on both the strength and deformation of rocks. On the other hand, the slope and peak of the curves of fractured rocks both increase as the confining pressure increases (Fig. 4b, d).
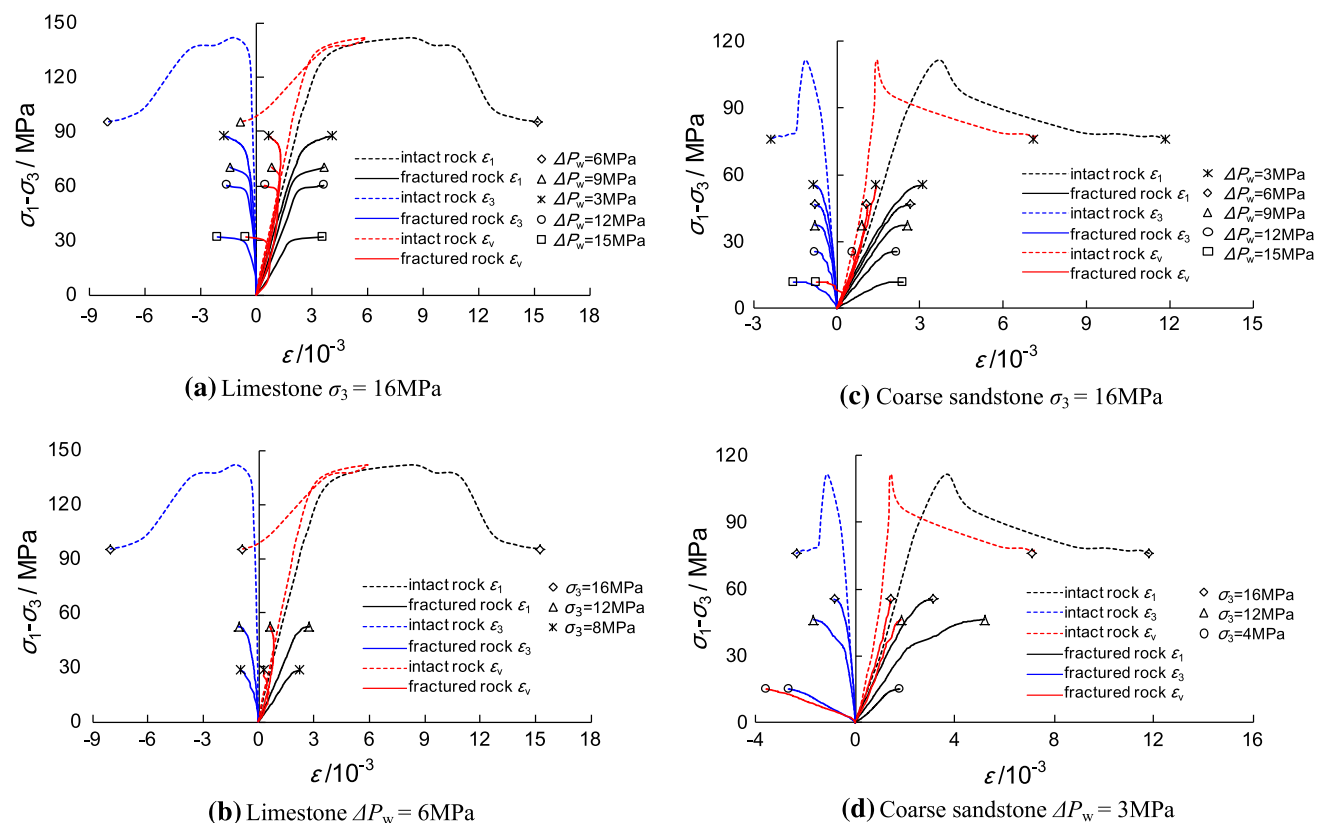

(a) Limestone $\sigma_3 = 16$MPa

(c) Coarse sandstone $\sigma_3 = 16$MPa

(b) Limestone $\Delta P_w = 6$MPa

(d) Coarse sandstone $\Delta P_w = 3$MPa

Fig. 4 Curves of stress–strain of rocks

Properties of deformation of fractured rocks

In order to reveal the weakening effect of differential water pressure on the deformation of fractured rocks and get the quantificational relationship between the deformation and differential water pressure, the changing trend of deformation modulus E_{50} and Poisson's ratio μ at the 50 % of the peak stress with differential water pressures are analyzed. The E_{50} and μ are both calculated with total stress by the reason of the complex distribution of pore pressures in the specimen under differential water pressures. As shown in the relationship curves of $E_{50}-\Delta P_w$ and $\mu-\Delta P_w$ under different confining pressures (Fig. 5), the deformation modulus E_{50} reduces with the increasing differential water pressure, but Poisson's ratio μ is just the opposite. Both the deformation modulus E_{50} and Poisson's ratio μ change as a parabola with the differential water pressure ΔP_w. The parabola equations are showed in Table 2. The slopes of the curves of $E_{50}-\Delta P_w$ and $\mu-\Delta P_w$ increase with the increasing differential water pressure but decrease as confining pressure increases. Hence it can be concluded that the weakening effect of higher water pressure on rocks' deformation is more significant, but on the other hand, the weakening effect of water pressures is severely restrained by confining pressures.

Properties of strength of fractured rocks

Figure 6 shows the relationship curves of the stress σ_1 calculated with total stress and the differential water pressure ΔP_w under different confining pressures. The strength reduces significantly with the increasing differential water pressure but increases when the confining pressure increases, which can be explained by the effective confining pressure (the difference between confining pressures and pore pressures generally) under the different water pressures. The increase of differential water pressures directly results in the reduction of effective confining pressures, thus affecting the strength of rocks. As shown in the equations in Fig. 6, the strength σ_1 has a good linear relationship with the differential water pressure ΔP_w.

Permeability of intact rock during the failure process

The permeability–strain curves of both limestone and coarse sandstone in the deformation and failure process are roughly in accord with the stress–strain curves (Fig. 7). The permeability evolution can be divided into the following several stages:

The permeability corresponding to OA segment of the stress–strain curve is very low. Because the damage degree of rocks in this stage is extremely low, the seepage channels are mainly the pore and micro-cracks whose connectivity is poor. For the limestone (Fig. 7a, c), because of the low porosity and the limits of the test conditions, the permeability of this stage is shown as zero in the figures and shows no obvious change in the test duration. In comparison, the coarse sandstone with the higher porosity shows more pronounced permeability (Fig. 7b, d). The permeability of coarse sandstone at this stage reduces firstly and increases later (Fig. 7d), which can be explained by the compaction of the pore and micro-cracks firstly and then the development of new damage under the increasing axial stress.

The permeability corresponding to AB segment of the stress–strain curve increases rapidly. During this stage, the cracks in the specimen develop rapidly and connect with each other, and the fractures become the main seepage channels. The permeability increases markedly due to the good connectivity of fractures. The peak permeability corresponds to the point B in the post-peak stress–strain curve, which indicates that the peak permeability always lags behind the peak stress.

The permeability corresponding to BC segment reduces gradually with the reducing stress and tends to be stable later in the residual phase. The reason is that the fractures continue
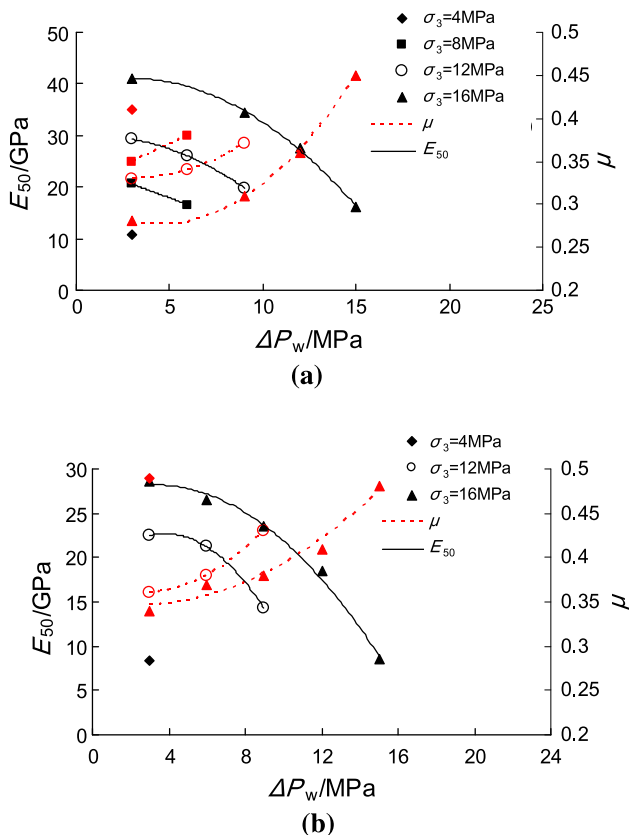

Fig. 5 Correlation curves of $E_{50}-\Delta P_w$ and $\mu-\Delta P_w$. **a** Limestone. **b** Coarse sandstone

Table 2 Equations of $E_{50}-\Delta P_w$ and $\mu-\Delta P_w$

Specimen	σ_3/MPa	$E_{50}-\Delta P_w$	$\mu-\Delta P_w$
Limestone	8	$E_{50} = -1.32\Delta P_w + 24.51$	$\mu = 0.01\Delta P_w + 0.32$
	12	$E_{50} = -0.1528\Delta P_w^2 + 0.2717\Delta P_w + 29.84$	$\mu = 0.0011\Delta P_w^2 - 0.0067\Delta P_w + 0.34$
	16	$E_{50} = -0.1685\Delta P_w^2 + 0.9734\Delta P_w + 39.678$	$\mu = 0.0016\Delta P_w^2 - 0.0146\Delta P_w + 0.31$
Coarse sandstone	12	$E_{50} = -0.315\Delta P_w^2 + 2.4083\Delta P_w + 18.1$	$\mu = 0.0017\Delta P_w^2 - 0.0083\Delta P_w + 0.37$
	16	$E_{50} = -0.1406\Delta P_w^2 + 0.9281\Delta P_w + 26.668$	$\mu = 0.0008\Delta P w^2 - 0.0036\Delta P_w + 0.35$
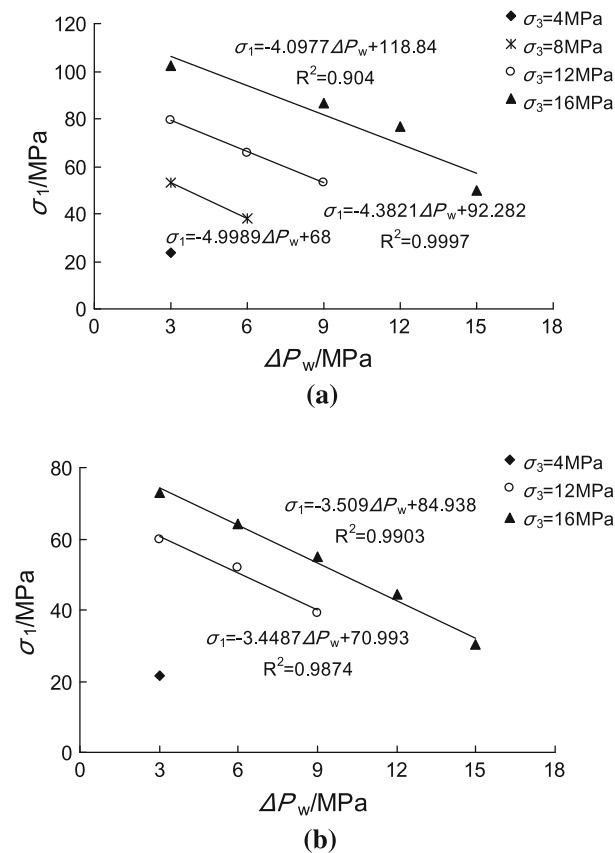
Fig. 6 Correlation curves of $\sigma_1-\Delta P_w$. **a** Limestone. **b** Coarse sandstone

to move slightly to lead to some compaction of the fractures during the post-peak softening stage and then the fractures tend to reach a new stable state at the residual phase.

At OA stage, damage is not significant in the rock and the water flows in the pore and original micro-cracks, so the permeability at this stage can be considered as the permeability of intact rocks. Figure 7 shows that the permeability at OA stage is much lower than that at the post-peak phase, where the specimen contains numerous fractures after damage. For the engineering rock masses which consist of fractures and intact rock, the permeability of the intact rock is extremely low compared with the fractures and the water mainly flows through the fractures, so the permeability of the engineering rock masses is primarily controlled by the permeability of the fractures.

Permeability of fractured rock

Permeability evolution in the deformation process

As with the intact rocks, the permeability–strain curves of fractured rocks have a close correlation with the stress–strain curves, whereas the permeability evolution of fractured rocks is different from that of intact rocks. As shown in Fig. 8, the permeability of fractured rocks reduces as the stress and strain increase before the yield stress, and then tends to be stable. The results indicate that fractures in the rock are compacted gradually during the stress–strain process.

As is known to us, the permeability of fractured rocks is closely related to the spatial geometric features of fractures such as fracture distribution. In order to reveal the spatial geometric features of the fractures in the rock specimen whose permeability changes following the above laws, Fig. 9 shows the photos of the fractured limestone and coarse sandstone. As shown in the photos, the main fractures intersect with the axial direction with a big angle and have obvious compression–shear characteristics. So the deformation characteristics that axial deformation is much greater than the lateral deformation and the permeability evolution that the permeability reduces with the increasing strain can be explained by the spatial geometric features of fractures which are significantly compacted under the axial stress.

Relationship between permeability and axial strain

In order to shed a new light on the relationship between the permeability and strain of fractured rocks with the fractures which have such spatial geometric features shown in Fig. 9, taking account of the deformation characteristics that the deformation in the axial direction is greater than that in the lateral direction and the volume of the specimen is mostly compressed, the correlation between the permeability and axial strain ε_1 before the yield stress is analyzed

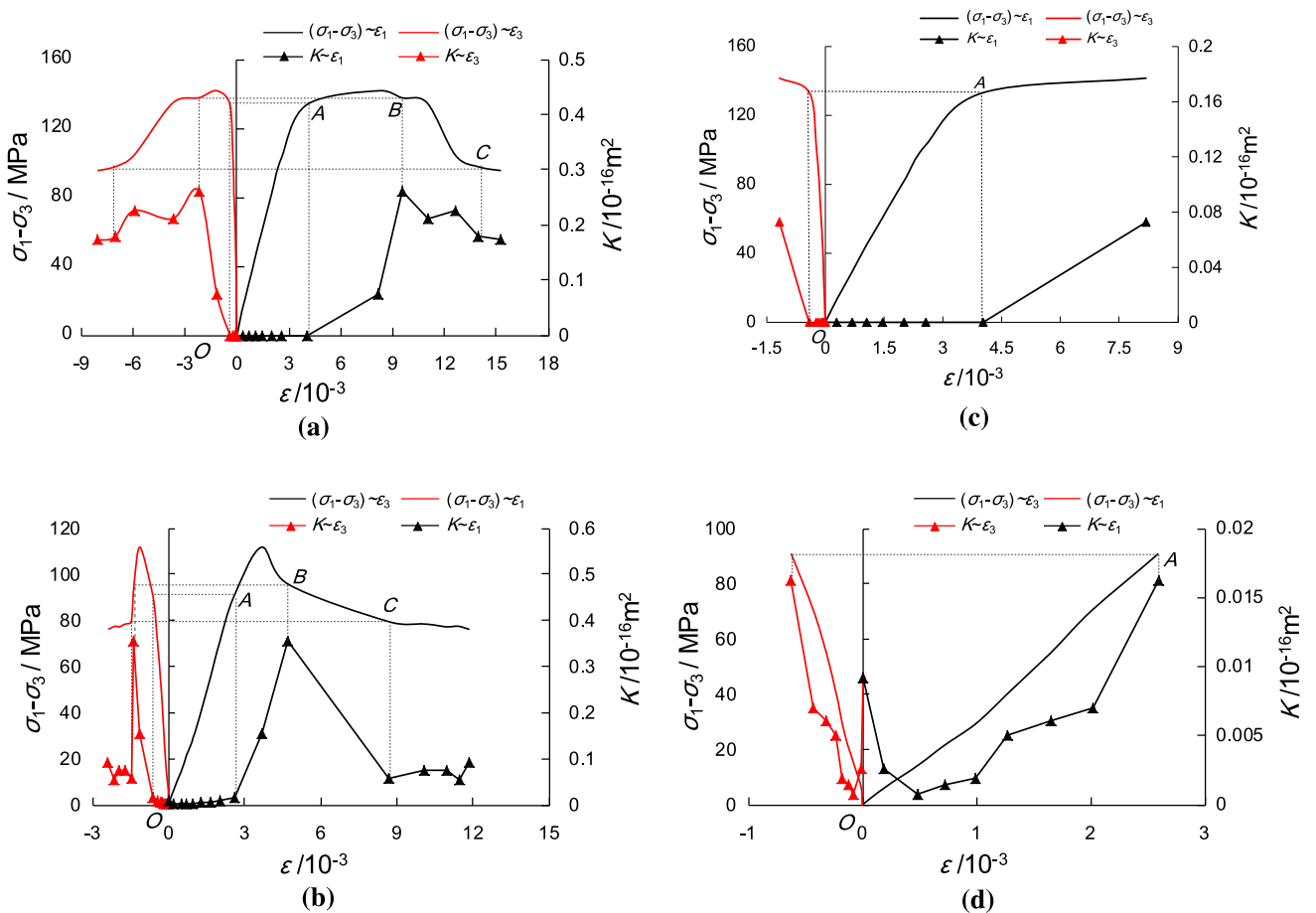**Fig. 7** Curves of permeability–strain and stress–strain of intact rocks. **a** Limestone σ_3 = 16MPa, ΔPw = 6MPa. **b** Coarse sandstone σ_3 = 16 MPa, ΔP_w = 3MPa. **c** *OA* curves of limestone. **d** *OA* curves of coarse sandstone

(Fig. 10). The results indicate that the permeability and axial strain ε_1 have a negative exponential relationship. The function is as follows:

$$K = \alpha e^{\beta \varepsilon_1} \qquad (1)$$

K in the function is the permeability; α and β in the function are the correlation coefficients; $\beta < 0$. The values of α and β under different confining pressures and differential water pressures are listed in Table 3, in which R^2 is the multiple correlation coefficient.

In the above equation, the value of α is the initial permeability of fractured rocks under the condition of $\sigma_1 = \sigma_3$. As shown in Fig. 11, the initial permeability increases with the increasing initial differential water pressure ΔP_w under a certain confining pressure, but reduces as the confining pressure σ_3 increases.

Relationship between permeability and stress

The permeability is not only related to the fracture distribution, but also significantly affected by the stress conditions

which have effects on the features of microstructures such as fracture apertures. Most researches have focused on the relationship between the permeability and normal stress, but the normal stress on the complex fractures cannot be obtained easily and accurately in engineering. So in this paper, the mean stress σ_m defined as $\sigma_m = (\sigma_1 + 2\sigma_3)/3$ is considered to represent the stress state of the fractured rocks and it is easy to get the value of σ_1 and σ_3 in engineering. The relationship between the permeability K and mean stress σ_m is analyzed and the result shows that the permeability reduces as the mean stress increases. So the relationship of power function between permeability K and mean stress σ_m is founded by the analysis of correlation between them (Figs. 12, 13). The function is as follows:

$$K = \gamma \sigma_m^{\eta} \qquad (2)$$

K in the function is the permeability; γ and η in the function are the correlation coefficients; $\eta < 0$.

The relationship of power function between permeability K and mean stress σ_m indicates that the permeability reduces very quickly under the low stress level and then the

(a) Limestone ΔP_w = 3MPa

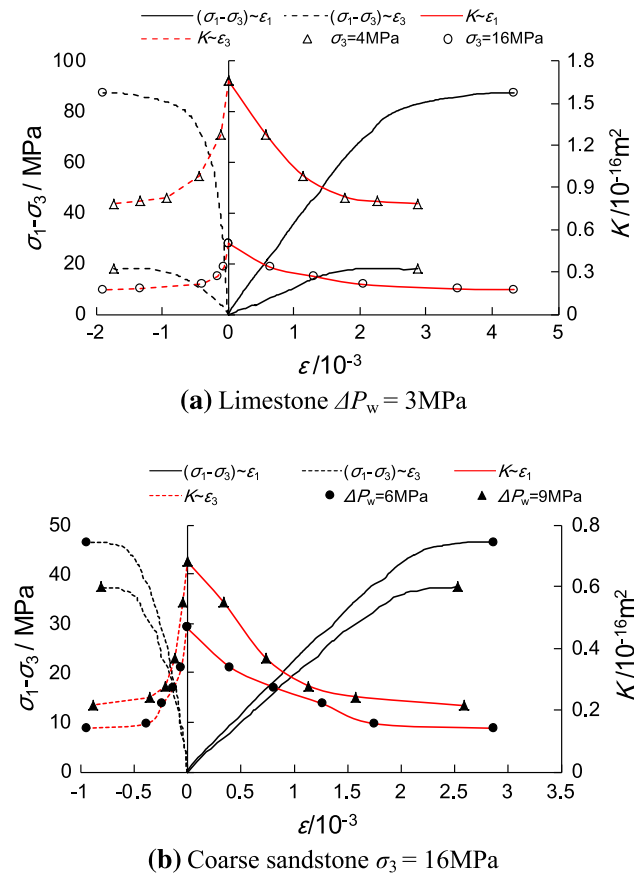

(b) Coarse sandstone σ_3 = 16MPa

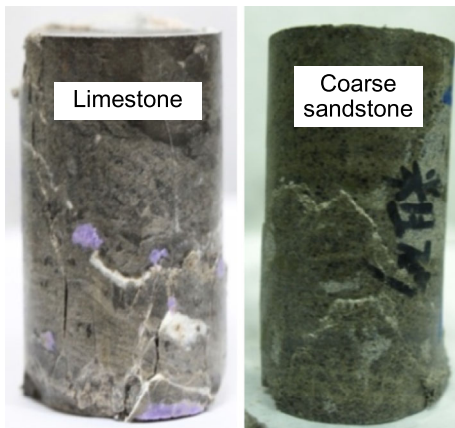**Fig. 8** Curves of permeability–strain and stress–strain of fractured rocks

Fig. 9 Photo of fractured rocks

reduction tends to be gentle. The permeability evolution with the mean stress is closely related to the deformation of fractures. The fracture aperture reduces significantly as the stress increases under lower stress level so that the permeability reduces sharply, while the fracture aperture has no obvious change under higher stress level so that the permeability tends to be stable.
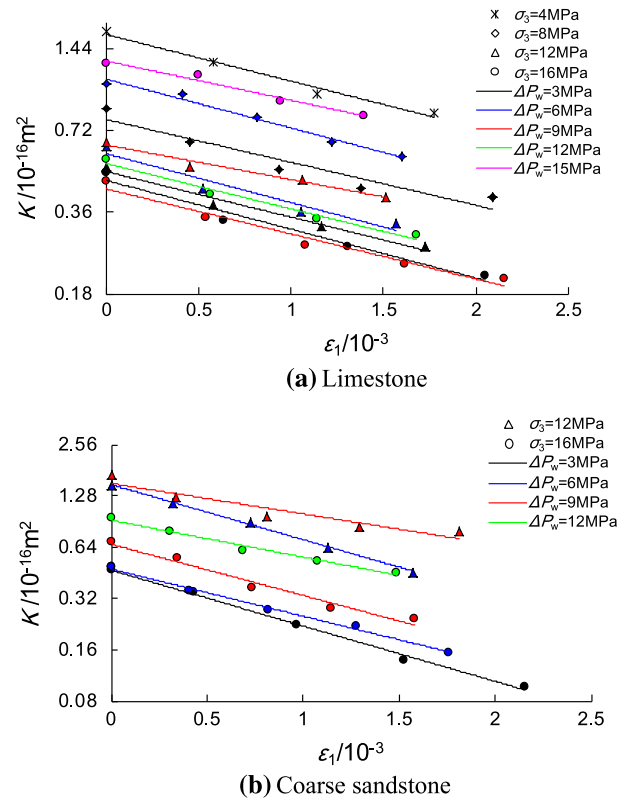

(a) Limestone

(b) Coarse sandstone

Fig. 10 Correlation curves of permeability–strain

Table 3 Correlation coefficients α and β of permeability K and axial strain ε_1

Specimen	σ_3/MPa	ΔP_w/MPa	α	β	R^2
Limestone	4	3	1.6198	−0.395	0.98
	8	3	0.7886	−0.363	0.91
	8	6	1.1097	−0.414	0.98
	12	3	0.5069	−0.386	0.98
	12	6	0.5901	−0.414	0.93
	12	9	0.6355	−0.293	0.97
	16	3	0.4705	−0.414	0.97
	16	9	0.4379	−0.382	0.97
	16	12	0.5422	−0.383	0.98
	16	15	1.2956	−0.334	0.97
Coarse sandstone	4	3	7.3046	−1.925	1.00
	12	3	1.4706	−0.545	1.00
	12	6	1.4892	−0.743	1.00
	12	9	1.5137	−0.412	0.90
	16	3	0.4664	−0.747	1.00
	16	6	0.4754	−0.636	1.00
	16	9	0.6651	−0.691	0.97
	16	12	0.9209	−0.498	0.98
	16	15	1.0832	−0.2	0.98
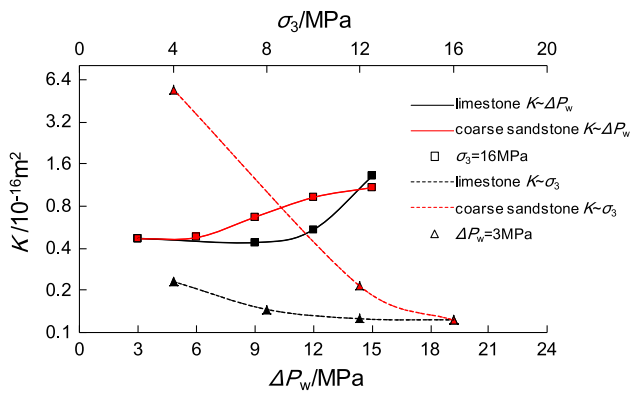
Fig. 11 Curves of $\alpha-\sigma_3$ and $\alpha-\Delta P_w$

(a)

(b)
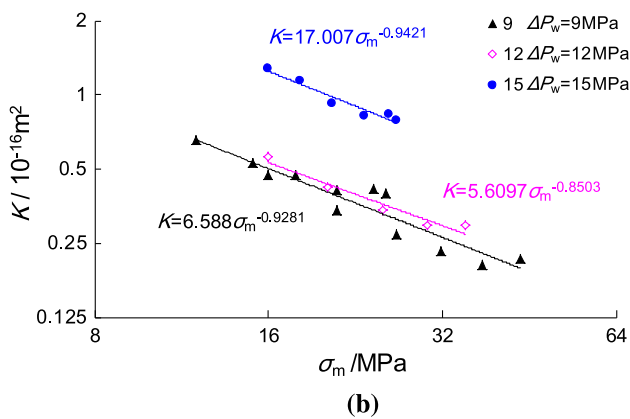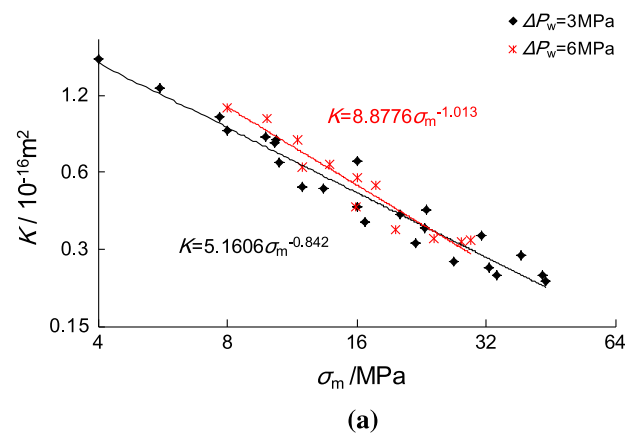
Fig. 12 Correlation curves of $K-\sigma_m$ of fractured limestone

(a)

(b)

Fig. 13 Correlation curves of $K-\sigma_m$ of fractured coarse sandstone

when the mean stress reaches or exceeds σ_{ml}. For fractured limestone, the proximate value of σ_{ml} is 30 MPa when the differential water pressure is 12 MPa or less and the value reaches 50 MPa when the differential water pressure reaches 15 MPa. For fractured coarse sandstone, the proximate value of σ_{ml} is 30 MPa when the differential water pressure is 3 MPa or less, but it becomes 40 MPa as the differential water pressure is in the range of 6–15 MPa.

Conclusions

The experimental researches on the mechanical characteristics and permeability of limestone and coarse sandstone from a coal mine during the stress–strain process have been performed and the results as follows are obtained:

1. The stress–strain curves and permeability evolution of intact rocks and that of fractured rocks are highly different. The stiffness and strength both reduce after the rock failure. The permeability of fractures rocks is much higher than that of intact rocks.

2. The differential water pressure which affects both the stress conditions and microstructures of fractured rocks has significant weakening effects on the mechanical

Based on the equations of the permeability and mean stress, the slopes of the $K-\sigma_m$ curves under different mean stresses are calculated and analyzed. The value of slope represents the reduction rate of the permeability with the mean stress. The reduction rate decreases when the mean stress increases and will be below 1 % at a certain mean stress which is defined as σ_{ml}. That means that the permeability of fractured rocks will have no obvious change
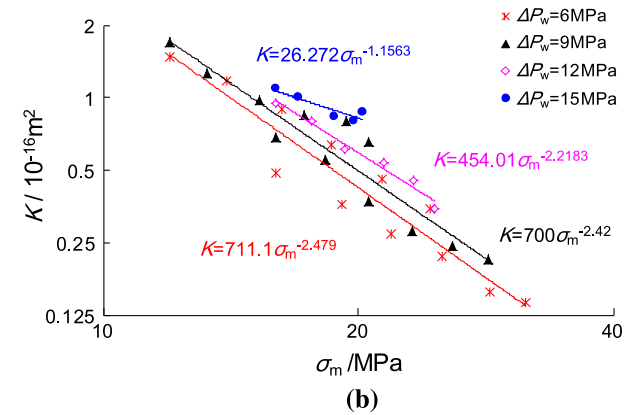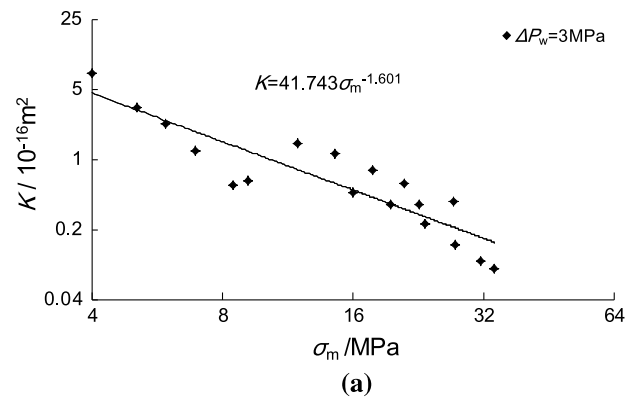
characteristics. The deformation modulus E_{50} reduces as a parabola with the differential water pressure ΔP_{w}, while Poisson's ratio μ increases as a parabola. The strength reduces linearly with the increasing differential water pressure.

3. The permeability of fractured rocks is closely related to the spatial geometric features of fractures. If the fractured rock contains the fractures which have obvious compression–shear features and are intersected by the axial stress with a big angle (as shown in Fig. 9), its permeability changes following a rule that the permeability reduces as the stress and strain increase and then tends to be sable gradually.

4. The permeability of such fractured rocks is closely related to the deformation and the stress conditions, and has a negative index correlation with the axial strain ε_1 and a power function correlation with the mean stress $\sigma_{\mathrm{m}}(\sigma_{\mathrm{m}} = (\sigma_1 + 2\sigma_3)/3)$. For fractured limestone and coarse sandstone, there is no significant change on the permeability when the mean stress reaches a certain value σ_{ml}.

References

Barton N, Bandis S, Bakhtar K (1985) Deformation and conductivity coupling of rock joints. Int J Rock Mech Min Sci Geomech Abstr 22(3):121–140

Brace WF, Walsh JB, Frangos WT (1968) Permeability of granite under high pressure. J Geophys Res 73(6):2225–2236

Chai B, Tong J, Jiang B et al (2014) How does the water–rock interaction of marly rocks affect its mechanical properties in the Three Gorges Reservoir area, China. Environ Earth Sci 72:2797–2810

Chang ZY, Zhao YS, Hu YQ et al (2004) Theoretic and experimental studies on seepage law of single fracture under 3D stresses. Chin J Rock Mech Eng 23(4):620–624 (in Chinese)

David C, Menendez B, Zhu W (2001) Mechanical compaction, microstructures and permeability in sandstones. Phys Chem Earth 26(1–2):45–51

Gale JE (1982) The effect of fracture type (induced versus natural) on the stress-fracture closure permeability relationships. In: Proc 23th Symp on Rock Mech, Berkeley

Gangi AF (1978) Variation of whole and fractured porous rock permeability with confining pressure. Int J Rock Mech Min Sci Geomech Abstr 15(5):249–257

Helland J, Raab S (2001) Experimental investigation of the differential stress on permeability of a lower Permian (Rotliegend) sandstone deformed in the brittle deformation field. Phys Chem Earth 26(1–2):33–38

Hsieh PA, Tracy JV, Neuzil CE et al (1981) A transient laboratory method for determining the hydraulic properties of 'tight' rocks-I. Theory. Int J Rock Mech Min Sci Geomech Abstr 18(3):245–252

Jiang ZQ, Ji LJ, Zuo RS et al (2002) Correlativity among rock permeability and strain, stress under servo-control condition. Chin J Rock Mech Eng 21(10):1442–1446 (in Chinese)

Jones FO (1975) A laboratory study of the effects of confining pressure on fracture flow and storage capacity in carbonate rock. J Petrol Technol 21(7):21–27

Kranzz RL, Frankel AD, Engelder CH et al (1979) The permeability of whole and jointed Barre granite. Int J Rock Mech Min Sci Geomech Abstr 16(4):225–234

Lajtai EZ, Schmidtke RH, Bielus LP (1987) The effect of water on the time-dependent deformation and fracture of a granite. Int J Rock Mech Min Sci Geomech Abstr 24(4):247–255

Li SP, Li YS, Li Y et al (1994) Permeability-strain equations corresponding to the complete stress–strain path of Yinzhuang sandstone. Int J Rock Mech Min Sci 31(4):383–391

Li SP, Wu DX, Xie WH et al (1997) Effect of confining pressure, pore pressure and specimen dimension on permeability of Yinzhuang sandstone. Int J Rock Mech Min Sci 34(3–4):435–441

Li JW, Xu J, Wang L et al (2013) Water–rock coupling test on mechanical properties of sandy slate rock mass. Chin J Geotech Eng 24(4):247–255 (in Chinese)

Masuda K (2001) Effect of water on rock strength in a brittle regime. J Struct Geol 23:1653–1657

Neuzil CE, Cooley C, Silliman SE et al (1981) A transient laboratory method for determining the hydraulic properties of 'tight' rocks-II. Theory. Int J Rock Mech Min Sci Geomech Abstr 18(3):253–258

Oda M, Takemura T, Aoki T (2002) Damage growth and permeability change in triaxial compression tests of Inada granite. Mech Mater 34:313–331

Peng SP, Meng ZP, Wang H et al (2003) Testing study on pore ratio and permeability of sandstone under different confining pressures. Chin J Rock Mech Eng 22(5):742–746 (in Chinese)

Tang CA, Tham LG, Lee PKK et al (2002) Coupled analysis of flow, stress and damage (FSD) in rock failure. Int J Rock Mech Min Sci 39:477–489

Vásárhelyi B, Ván P (2006) Influence of water content on the strength of rock. Eng Geol 84:70–74

Walsh JB (1981) Effect of pore pressure and confining pressure on fracture permeability. Int J Rock Mech Min Sci Geomech Abstr 18(5):429–435

Wang JA, Park HD (2002) Fluid permeability of sedimentary rocks in a complete stress–strain process. Eng Geol 63:291–300

Wang HL, Xu WY (2013) Relationship between permeability and strain of sandstone during the process of deformation and failure. Geotech Geol Eng 31:347–353

Wang HL, Xu WY, Shao JF (2014) Experimental researches on hydro-mechanical properties of altered rock under confining pressure. Rock Mech Rock Eng 47:485–493

Wasantha PLP, Ranjith PG (2014) The Taguchi approach to the evaluation of the influence of different testing conditions on the mechanical properties of rock. Environ Earth Sci 72:79–89

Zhang R, Jiang ZQ, Sun Q et al (2013) The relationship between the deformation mechanism and permeability on brittle rock. Nat Hazards 66:1179–1187

Zhu W, Wong TF (1996) Permeability reduction in a dilating rock: network modeling of damage and tortuosity. Geophys Res Lett 23(22):3099–3102

Zoback MD, Byerlee JD (1975) The effect of microcrack dilatancy on the permeability of westerly granite. J Geophys Res 80(5):752–755